MITSUBISHI ELECTRIC RESEARCH LABORATORIES
https://www.merl.com

Kernel Regression for Energy-Optimal Control of Fully Electric Vehicles

Menner, Marcel; Di Cairano, Stefano

TR2021-132 November 13, 2021

Abstract

This paper presents a control algorithm for electric vehicles (EVs) with multiple motors. The control algorithm minimizes the EV's energy usage by optimizing the efficiency of its electric motors. The degrees of freedom exploited by the control algorithm are the torque-split ratio between multiple motors, the gear ratio for transmission, as well as the velocity profile of the EV. The algorithm uses kernel regression to learn a pseudo-convex cost function for optimal control from tabulated data of the electric motors' efficiency maps. The main advantages of the algorithm are its real-time feasibility due to the pseudo-convex shape and its flexible approximation capabilities. A simulation study shows how an EV with multiple but different motors and a torque-split controller can efficiently exploit the range of operation of the individual motors. The proposed algorithm achieves energy savings of up to 20% and 40% for the US06 and Urban Dynamometer Driving Schedule (UDDS), respectively, by leveraging the strengths of the different electric motors. Finally, we show that the energy-optimal velocity profile varies for different EV specifications as a result of their motor efficiencies. In particular, compared to a profile with constant acceleration, the proposed kernel regression algorithm achieves energy savings of up to 13%.

IEEE Vehicle Power and Propulsion Conference 2021

Mitsubishi Electric Research Laboratories, Inc.
201 Broadway, Cambridge, Massachusetts 02139

Kernel Regression for Energy-Optimal Control of Fully Electric Vehicles

Marcel Menner and Stefano Di Cairano

Abstract— **This paper presents a control algorithm for electric vehicles (EVs) with multiple motors. The control algorithm minimizes the EV's energy usage by optimizing the efficiency of its electric motors. The degrees of freedom exploited by the control algorithm are the torque-split ratio between multiple motors, the transmission gear ratio, as well as the velocity profile of the EV. The algorithm uses kernel regression to learn a pseudo-convex cost function for optimal control from tabulated data of the electric motors' efficiency maps. The main advantages of the algorithm are its real-time feasibility due to the pseudo-convex shape and its flexible approximation capabilities. A simulation study shows how an EV with multiple but different motors and a torque-split controller can efficiently exploit the range of operation of the individual motors. The proposed algorithm achieves energy savings of up to 20% and 40% for the US06 and Urban Dynamometer Driving Schedule (UDDS), respectively, by leveraging the strengths of the different electric motors. Finally, we show that the energy-optimal velocity profile varies for different EV specifications as a result of their motor efficiencies. In particular, compared to a profile with constant acceleration, the proposed kernel regression algorithm achieves energy savings of up to 13%.**

I. Introduction

Electric vehicles (EVs) are becoming increasingly popular as they have the potential to decrease pollutant emissions of automobiles and to be powered by renewable energy sources. Improving the energy efficiency (and, in turn, an EV's range) make an EV cheaper to operate, more environmentally friendly, and more attractive to a broader range of customers. The efficiency of an electric motor (EM) is a function of its operating point, i.e., the torque and the rotational speed [1]. As a result, for energy-optimal control of EVs, the EMs' efficiencies as a function of their operating point need to be considered. However, in order to exploit the varying motor efficiencies, we need (i) degrees of freedom in the EV architecture such that the overall range of operating point can be best exploited and (ii) a fast control algorithm that can utilize these degrees of freedom for energy-optimal control. For example, an EV with one powerful motor and one weaker motor can allocate the torque demand such that the weaker motor is utilized for cruise conditions and the more powerful motor is used for peak torque demands.

In this paper, we propose an algorithm for energy-optimal control of EVs. The control algorithm exploits the available degrees of freedom such as the torque-split ratio between motors (for EVs with multiple motors), the transmission gear (for EVs with continuously variable transmissions (CVTs)), as well as the velocity profile to be tracked. The algorithm does not need all of these degrees of freedom to operate, e.g., for EVs with four in-wheel motors, the torque-split controller determines how much torque is to be exerted by each motor and does not require a transmission controller. The control algorithm uses tabulated data of motor efficiencies in order to learn a cost function that can be used for optimal control. In particular, we use kernel regression to learn a differentiable and pseudo-convex cost function, which includes both driving losses and losses caused by motor efficiencies. The cost function includes both driving modes using and regenerating energy. The pseudo-convex shape and differentiability makes the optimization real-time feasible, whereas the kernel function flexibility is important to accurately represent the losses of the EV. Simulation results show that an EV with two EM and one CVT can save up to 20% and 40% for the US06 and UDDS driving schedules, respectively, compared to a configuration with only one EM and fixed gear. Furthermore, we show that an additional 2%–13% of energy can be saved by optimizing the velocity profile over a short horizon.

Related Work: Energy management strategies for hybrid EVs have been studied in the literature, e.g., in [2]–[11], where the main goal is to find a torque (or power)-split strategy between an EM and an internal combustion engine to optimally operate the vehicle. For example, [2] presents a model-based strategy for the real-time power-split control of parallel hybrid EVs. In [5], a model predictive controller is used for energy management. In [6], a predictive model for the driver behavior based on a Markov chain is used to optimally allocate the power request. Further, [12] presents a survey on utilizing driver predictions for energy management. In [7] a method to solve the energy management problem with engine start and gearshift costs is presented, which is based on a combination of dynamic programming and convex optimization. In [8], an engine on/off switching strategy based on convex optimization is presented.

Recently, there has been increased interest in fully electric vehicles, see, e.g., [13]–[18]. In [13], a control strategy to maintain stability and improve handling of a four-wheel independently actuated EV is presented. In [14], convex optimal control is used to optimize the efficiency of a battery-assisted trolley bus. Similarly to our work, [15] considers motor efficiency maps for EVs, and uses an evaluation index and a control logic. In contrast, here we use a kernel-based model shaped as pseudo-convex function that can be used for gradient-based optimization. In addition, we propose an algorithm that uses the motor efficiencies for optimizing the velocity profile. In [16], the problem of switching between different drive modes of electric drive system is considered,

All authors are with Mitsubishi Electric Research Laboratories (MERL), Cambridge, MA, 02139, USA (e-mail: menner@ieee.org; dicairano@ieee.org).

with the objective of optimizing the efficiency of electric busses. In [17], independently-actuated wheels are utilized for EV chassis control to improve passenger comfort. In [18], particle swarm optimization with a torque-split strategy is utilized to save energy for a dual-motor powertrain.

II. Mathematical Cost Function Model

We present an algorithm that uses tabulated data to learn a cost function used for optimal control. The algorithm uses kernel regression and constraints that render the cost function pseudo-convex. The rationale for using kernel regression is that the resulting cost function is differentiable and offers very flexible approximation capabilities. Further, the pseudo-convex shape ensures that there is only one global optimum, which is beneficial for gradient-based optimization.

Kernel regression is a non-parametric technique that is intimately intertwined with Gaussian processes [19]. It is a paradigm that learns a function/mapping, $y = L(\boldsymbol{x})$, and uses a set of training data,

$$\boldsymbol{X} = \begin{bmatrix}\boldsymbol{x}_1 & \boldsymbol{x}_2 & \dots & \boldsymbol{x}_N\end{bmatrix} \in \mathbf{R}^{n_x \times N} \tag{1a}$$

$$\boldsymbol{y} = \begin{bmatrix}y_1 & y_2 & \dots & y_N\end{bmatrix} \in \mathbf{R}^{1 \times N}, \tag{1b}$$

where a perfect function would yield $y_i = L(\boldsymbol{x}_i)$ for all $i = 1, ..., N$, where N is the number of training data points. We use $y = L(\boldsymbol{x}) = \boldsymbol{k}(\boldsymbol{x}, \boldsymbol{X})\boldsymbol{\alpha} + \alpha_0$ with

$$\boldsymbol{k}(\boldsymbol{x}, \boldsymbol{X}) = \begin{bmatrix}k(\boldsymbol{x}, \boldsymbol{x}_1) & k(\boldsymbol{x}, \boldsymbol{x}_2) & \dots & k(\boldsymbol{x}, \boldsymbol{x}_N)\end{bmatrix}, \tag{2}$$

where $k(\cdot, \cdot)$ denotes a kernel function, and $\boldsymbol{\alpha}$ and α_0 are the weights to be learned using the training data. Let

$$\boldsymbol{K}(\boldsymbol{X}, \boldsymbol{X}) = \begin{bmatrix}\boldsymbol{k}(\boldsymbol{x}_1, \boldsymbol{X}) \\ \boldsymbol{k}(\boldsymbol{x}_2, \boldsymbol{X}) \\ \vdots \\ \boldsymbol{k}(\boldsymbol{x}_N, \boldsymbol{X})\end{bmatrix}.$$

We learn the weights, $\boldsymbol{\alpha}$ and α_0, using the following optimization problem

$$\min_{\alpha_0, \boldsymbol{\alpha} \in \mathbf{R}^{n_x}} \quad \left\|(\sigma^2 \boldsymbol{I} + \boldsymbol{K}(\boldsymbol{X}, \boldsymbol{X}))\boldsymbol{\alpha} + \mathbf{1}\alpha_0 - \boldsymbol{y}^T\right\|_2^2 \tag{3a}$$

$$\text{s.t. } \langle \nabla_{\boldsymbol{x}} \boldsymbol{k}(\boldsymbol{x}, \boldsymbol{X})\boldsymbol{\alpha}, \boldsymbol{x} - \boldsymbol{x}^\star \rangle \geq 0 \quad \forall \boldsymbol{x} \in \mathcal{X}, \tag{3b}$$

where $\mathbf{1} = [1\ 1\ \dots\ 1]^T \in \mathbf{R}^N$, $\langle \cdot, \cdot \rangle$ denotes the inner product, $\boldsymbol{I}$ is the identity matrix, and σ is used to account for noisy training data. Eq. (3b) ensures that there is only one global optimum, $\boldsymbol{x}^\star$, by ensuring that the resulting function is pseudo-convex for all $\boldsymbol{x} \in \mathcal{X}$, where the set $\mathcal{X}$ could be, e.g., the operating range. Note that (3) requires the choice of an optimum, $\boldsymbol{x}^\star$. The optimization problem in (3) is convex in α_0 and $\boldsymbol{\alpha}$. The main idea in this work is to use the kernel regression technique to learn a continuous function from tabulated data (1). For example, we learn the motor efficiency, η, as a function of motor speed, ω, and torque, τ, with $\eta = \boldsymbol{k}([\omega,\ \tau]^T, \boldsymbol{X})\boldsymbol{\alpha} + \alpha_0$. The reader is referred to [19] for more details on regression and kernels.

Remark 1: Throughout, we use the squared-exponential kernel, $k(\boldsymbol{x}_1, \boldsymbol{x}_2) = \nu^2 \exp\left(-\frac{1}{2l^2}\|\boldsymbol{x}_1 - \boldsymbol{x}_2\|_2^2\right)$, where l is the length scale and ν^2 is the output variance. This kernel offers the advantage of a vanishing gradient for $\boldsymbol{x}$ far away from the training data, $\boldsymbol{X}$.

Remark 2: We use normalized training data $\boldsymbol{X} \in [0, 1]^{n_x \times N}$ and $\boldsymbol{y} \in [0, 1]^{1 \times N}$ to avoid hyper-parameter tuning for different scales. Throughout, we choose $l = 0.1$, $\nu = 1$, $\sigma = 0.1$. It is possible to perform hyper-parameter optimization to improve the model fit, as in Bayesian optimization [19].

III. Energy-Optimal Control Strategy

We consider the longitudinal motion model of an EV,

$$ma_k = -F_{\text{drag}}(v_k) - F_{\text{roll}}(v_k) + \tfrac{1}{r_{\text{wheel}}} T_k \tag{4a}$$

$$F_{\text{drag}}(v_k) = \tfrac{1}{2} c_{\text{drag}} A_{\text{drag}} \rho_{\text{air}} v_k^2 \tag{4b}$$

$$F_{\text{roll}}(v_k) = \text{sign}(v_k) c_{\text{roll}} mg, \tag{4c}$$

where m is the mass, a_k and v_k are the acceleration and velocity at time step k, respectively, $F_{\text{drag}}(v_k)$ and $F_{\text{roll}}(v_k)$ are the aerodynamic drag and rolling resistance, respectively, c_{roll} is the roll coefficient, c_{drag} is the drag coefficient, A_{drag} is the frontal area, g is the gravity, and ρ_{air} is the air density. The axles' inertia and road grade may also be included. The total wheel torque is T_k and the wheel radius is r_{wheel}, where T_k and the EV velocity are related to the torques and the speeds of the n_{EM} motors by

$$T_k = q_k^1 \tau_k^1 + q_k^2 \tau_k^2 + \ldots + q_k^{n_{\text{EM}}} \tau_k^{n_{\text{EM}}} \tag{4d}$$

$$v_k = \tfrac{r_{\text{wheel}}}{q_k^1} \omega_k^1 = \tfrac{r_{\text{wheel}}}{q_k^2} \omega_k^2 = \ldots = \tfrac{r_{\text{wheel}}}{q_k^{n_{\text{EM}}}} \omega_k^{n_{\text{EM}}}, \tag{4e}$$

where q_k^i is the gear ratio between motor i and the wheels, and τ_k^i and $\omega_k^i \geq 0$ are the torque and speed of motor i.

In this paper, we consider power losses that originate from aerodynamic drag and from rolling resistance, as well as power losses due to efficiencies of the EMs,

$$L_{\text{EV}}(v_k, \boldsymbol{z}_k) = v_k(F_{\text{drag}}(v_k) + F_{\text{roll}}(v_k)) \tag{5a}$$

$$+ \sum_{i=1}^{n_{\text{EM}}} L_{\text{EM}i}(\omega_k^i, \tau_k^i), \tag{5b}$$

where L_{EV} is the total loss of the EV, $L_{\text{EM}i}$ is the loss of motor i as a function of the motor's states, ω_k^i and τ_k^i, and $\boldsymbol{z}_k = [\omega_k^1\ \tau_k^1\ \omega_k^2\ \tau_k^2\ \dots\ \omega_k^{n_{\text{EM}}}\ \tau_k^{n_{\text{EM}}}]^T \in \mathbf{R}^{2n_{\text{EM}}}$. The motor losses $L_{\text{EM}i}(\omega_k^i, \tau_k^i) \geq 0$ are a function of the motor speed and torque, $\eta^i(\omega_k^i, \tau_k^i) \in [0\ 1]$, with

$$L_{\text{EM}i}(\omega_k^i, \tau_k^i) = \begin{cases}\omega_k^i \tau_k^i \left(\frac{1}{\eta^i(\omega_k^i, \tau_k^i)} - 1\right) & \text{if } \tau_k^i \geq 0 \\ \omega_k^i \tau_k^i \left(\eta^i(\omega_k^i, \tau_k^i) - 1\right) & \text{else.}\end{cases} \tag{6}$$

However, since motor efficiencies are often in the form of tabulated data rather than a continuous function, we learn $\eta^i(\omega^i, \tau^i)$ and L_{EV} in (5) using kernel regression, which is outlined in the following.

Remark 3: For simplicity, we do not consider EVs driving in reverse. Hence, $\omega_k^i \geq 0$ and $v_k \geq 0$. However, we allow the EMs to regenerate energy, i.e., $\tau_k^i < 0$.

A. Energy-Conscious Velocity Profile Optimization Problem

In this paper, we want to minimize the losses in (5) subject to the constraints on the vehicle dynamics in (4),

$$\min_{v_k,a_k,\boldsymbol{z}_k} \sum_{k=0}^{N_{\mathrm{VP}}} L_{\mathrm{EV}}(v_k,\boldsymbol{z}_k) \tag{7a}$$

$$\text{s.t. } v_{k+1} = v_k + T_s a_k \qquad \forall\ k = 0,...,N_{\mathrm{VP}} \tag{7b}$$

$$c_{\mathrm{profile,eq}}(v_k,a_k) = 0 \tag{7c}$$

$$c_{\mathrm{profile,ineq}}(v_k,a_k) \leq 0 \tag{7d}$$

$$\text{motion model (4)} \tag{7e}$$

$$c_{\mathrm{EM,eq}}(\omega_k^i,\tau_k^i) = 0 \qquad \forall\ i = 0,...,n_{\mathrm{EM}} \tag{7f}$$

$$c_{\mathrm{EM,ineq}}(\omega_k^i,\tau_k^i) \leq 0, \tag{7g}$$

where N_{VP} is the horizon of the velocity profile optimization, (7c) and (7d) encode specifications for the velocity profile, and (7f) and (7g) encode constraints on the EMs. Eq. (7) is a predictive control problem to be implemented in receding horizon fashion similar to model predictive control. While (7) may be a highly nonlinear problem, we can make a simplifying assumption that significantly reduces the computational requirements.

B. Sequential Procedure for Energy-Optimal Control

In order to solve (7) with the limited computing capabilities of automotive-grade microcontrollers, we assume that the EM dynamics are fast compared to the vehicle dynamics. This implies that (7f) and (7g) do not affect the resulting velocity profile. Then, we solve (7) by a sequential approach that consist of a transmission controller, a torque-split controller, and a velocity profile optimizer. The three modules are detailed in Section III-B.1–III-B.3 and control the EMs as follows. First, the velocity profile optimizer generates an energy-optimal torque and speed profile. Second, the torque-split controller uses the torque and speed profile to compute an optimal torque-split ratio between the EMs. Third, the transmission controller uses the torque-split ratio as well as the vehicle speed in order to compute the optimal gear ratios. The learning procedure for the three modules is reversed due to dependencies, e.g., for learning the optimal torque-split ratio, the optimal gear ratios for specific torques are used.

1) Transmission controller: If the EV has a CVT, the gear ratio is optimized (for each CVT) based on a given torque and speed demand, τ_k^i and ω_k, i.e.,

$$q_k^i = \arg\max_{\tilde{q}}\ \eta^i\left(\tilde{q}\omega_k^i, \tau_k^i\right). \tag{8}$$

We learn $\eta^i(\omega^i,\tau^i)$ using the kernel-based regression method in Section II with the training data

$$\boldsymbol{x}_j = \begin{bmatrix}\omega_j & \tau_j\end{bmatrix}^T, \quad y_j = \eta_j,$$

where ω_j, τ_j, and η_j are the data points from the EM's efficiency map. We need to impose "$\leq$" rather than "$\geq$" in (3b), due to maximizing the efficiency rather than minimizing losses. Additionally, we choose $\boldsymbol{x}^\star = [\omega_j^\star\ \tau_j^\star]^T$ with $\{\omega_j^\star,\ \tau_j^\star\} = \arg\max_j\ \eta(\omega_j,\tau_j)$, i.e., the operating point of maximum efficiency in the training data, and impose $\alpha_0 = 0$, which implies that the efficiency $\eta \to 0$ for ω,τ faraway from the EM's operating range by the properties of the squared exponential kernel.

Remark 4: This step is unnecessary for EVs without a CVT. For transmissions with fixed gears, this step consists of choosing the gear ratio, which yields the highest efficiency for the specific power demand.

2) Torque-split controller: We use the efficiencies that result from (8) to determine the optimal torque-split ratio between multiple motors, given torque and wheel speed demand for the EV, T_k and ω_k in (4). The result is a function that provides the optimal allocation of torque demand among the EMs, given an overall torque and vehicle speed demand,

$$\begin{bmatrix}\tau_k^1 & \tau_k^2 & \dots & \tau_k^{n_{\mathrm{EM}}}\end{bmatrix} = \mathrm{TS}_{\boldsymbol{\Omega},\boldsymbol{T}}(\omega_k, T_k), \tag{9}$$

where $\mathrm{TS}_{\boldsymbol{\Omega},\boldsymbol{T}}$ is a function that outputs the torque-split ratio by interpolating ω_k and T_k using the training data $\boldsymbol{\Omega} = \{\bar{\omega}_1,\bar{\omega}_2,\dots,\bar{\omega}_{n_\Omega}\}$ and $\boldsymbol{T} = \{\bar{\tau}_1,\bar{\tau}_2,\dots,\bar{\tau}_{n_T}\}$. We obtain the function $\mathrm{TS}_{\boldsymbol{\Omega},\boldsymbol{T}}$ using the following training procedure. First, we create the training set $\boldsymbol{\Omega}$ and $\boldsymbol{T}$ using evenly-spaced data points. Then, for every combination $\bar{\omega}_j,\bar{\tau}_j$ we compute the energy-optimal torque-split ratio using η^i in (8) for all EM $i = 1,\dots,n_{\mathrm{EM}}$. This procedure is done offline and hence does not need to be real-time feasible.

Remark 5: This step is unnecessary for EVs with one EM.

3) Velocity profile optimization: For this step, we use (4) in order to express the cost function (7a) in terms of the vehicle velocity and acceleration,

$$\begin{bmatrix}\omega_k\\ T_k\end{bmatrix} = \begin{bmatrix}\frac{1}{r_{\mathrm{wheel}}} v_k\\ r_{\mathrm{wheel}}(ma_k + F_{\mathrm{drag}}(v_k) + F_{\mathrm{roll}}(v_k))\end{bmatrix}. \tag{10}$$

This allows us to consider the nonlinear vehicle dynamics through the cost function and removes the need to enforce nonlinear constraints. Thus, we obtain

$$\min_{v_k,a_k} \sum_{k=0}^{N_{\mathrm{VP}}} L_{\mathrm{EV}}(v_k,a_k) \tag{11a}$$

$$\text{s.t. } v_{k+1} = v_k + T_s a_k \quad \forall\ k = 0,...,N_{\mathrm{VP}} \tag{11b}$$

$$c_{\mathrm{profile,eq},k}(v_k,a_k) = 0 \tag{11c}$$

$$c_{\mathrm{profile,ineq},k}(v_k,a_k) \leq 0 \tag{11d}$$

with cost function

$$L_{\mathrm{EV}}(v_k,a_k) = v_k(F_{\mathrm{drag}}(v_k) + F_{\mathrm{roll}}(v_k)) + L_{\mathrm{EM}}(v_k,a_k),$$

where $L_{\mathrm{EM}}(v_k,a_k)$ comprises all drivetrain losses and the loss function in (11a) differs from (7a) by virtue of its inputs. Finally, we learn the cost function in (11a) using the method in Section II with the training data

$$\boldsymbol{x}_j = \begin{bmatrix}v_j & a_j\end{bmatrix}^T,$$
$$y_j = v_j(F_{\mathrm{drag}}(v_j) + F_{\mathrm{roll}}(v_j)) + L_{\mathrm{EM}}(v_j,a_j),$$

where $L_{\mathrm{EM}}(v_j,a_j)$ is obtained by sequentially solving (10), (9), and then (8). Additionally, we choose $\boldsymbol{x}^\star = [v_j\ a_j]^T = [0\ 0]^T$ in (3), which is an obvious choice as the vehicle's losses are $L_{\mathrm{EV}}(0\ \mathrm{m/s}, 0\ \mathrm{m/s^2}) = 0$. Fig. 1 shows examples

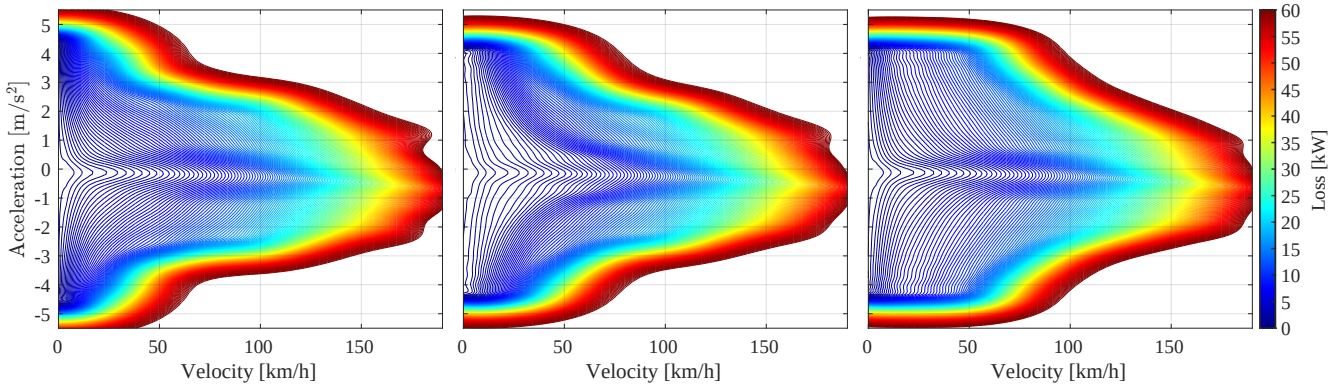

Fig. 1. Contour plot of electric vehicle losses, as function of vehicle velocity and acceleration. The levels are at 300 W increments. The EV has two EMs with maximum power 150 kW and 50 kW. Left: No CVTs. Middle: 50 kW motor with CVT. Right: 150 kW motor with CVT. The differences between the loss functions show that the configuration of the EV, i.e., multiple motors and/or CVTs, impacts the control decisions for optimizing energy consumption.

of the cost in (11a) as functions of the EV's velocity and acceleration for different EV architectures.

Remark 6: For driving tasks with a completely fixed torque and speed demand, we do not need to solve (11). However, for energy efficiency, it still makes sense to compute the optimal torque-split ratio, as well as the optimal gear ratios for the EMs, which we will show in Section IV.

4) Overall learning and control procedure: Algorithm 1 summarizes the offline training and the online application of the proposed control algorithm. First, we learn $\eta^i(\omega^i, \tau^i)$ in (8) using data from the motor's efficiency map. Second, we learn the torque-split function in (9) using (8). Finally, we learn the function L_{EM} in (11a) using the mapping in (10), the torque-split function in (9), and (8). For control, the order is reversed. First, we solve (11) for the optimal velocity and acceleration profile, which are used to compute the required wheel speed and torque with (10). Next, the wheel speed and torque are used to determine the optimal torque-split ratio with (9). Finally, given the allocated torque for each EM, we determine the optimal gear ratios with (8).

Algorithm 1: Training and control procedure

1 **Offline Training**;
2 Learn $\eta^i,\ \forall i = 1, ..., n_{\mathrm{EM}}$, with method in Section II;
3 Learn $\mathrm{TS}_{\boldsymbol{\Omega},\boldsymbol{T}}$ in (9);
4 Learn L_{EV} in (11) with method in Section II;
5 **Online Energy Optimization**;
6 Solve (11);
7 Obtain ω_k, T_k from (10);
8 Determine torque-split ratio from (9);
9 Determine transmission gear from (8);

IV. Results

We consider a passenger EV with longitudinal dynamics (4), with the parameters in Table I. For clarity of presentation, we consider EV configurations with two motors, $n_{\mathrm{EM}} = 2$. Furthermore, we model all transmissions to not incur any losses, i.e., 100% efficiency. However, the method in this paper can easily incorporate any number of EMs, e.g., four in-wheel motors, and other drive-train losses, e.g., in a CVT.

TABLE I
Vehicle Parameters

Type	Symbol	Value
EV mass (incl. weight of motors) + CVT mass	m	1500 kg + 100 kg per CVT
Wheel radius	r_{wheel}	0.3 m
Roll coefficient	c_{roll}	0.01
Drag coefficient	c_{drag}	0.3
Frontal area	A_{drag}	0.3 m^2
Air density	ρ_{air}	1.225 kg/m^3
Gravitational force	g	9.81 m/s^2

Electric motor model: We use the motor specifications provided in the QuasiStatic Simulation (QSS) toolbox [1]. In order to study a range of different motor specifications, we scale the torque values of the efficiency table. This choice of motor data makes the results in this paper reproducible. Furthermore, the data are sufficient to illustrate and analyze the algorithm in this paper.

A. Fixed Torque and Speed Demand — Driving Schedules

First, we show how much energy can be saved by exploiting the degrees of freedom in the motor control using the algorithm in this paper. In particular, we investigate energy savings of multiple EMs and CVTs with a torque-split strategy. For reproducibility and comparability, we use two commonly-used driving schedules, UDDS and US06 [20].

Impact of torque-split controller: Fig. 2 illustrates a comparison of EV architectures without a CVT but with two EMs, whose maximum powers sum up to 200 kW, i.e., the maximum power of motor 1 is $P_1 = 200\ \mathrm{kW} - P_2$. It shows that a suitable choice of EMs with a torque-split controller can exploit the range of operation of the individual motors more efficiently and save up to 18% when driving the US06 and 30% for UDDS, compared to an EV with one EM with maximum power of 200 kW. Intuitively, it makes sense to have an EV with one less powerful motor, which operates efficiently under cruising conditions, and one more powerful motor to be used for higher torque demand. Here, we found

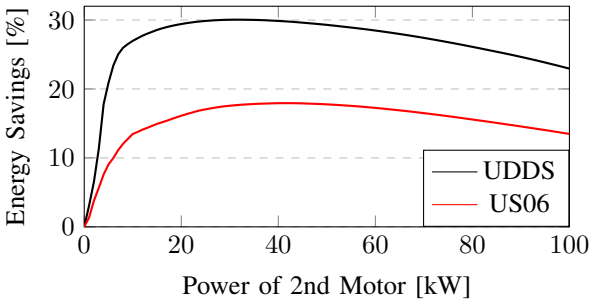

Fig. 2. Impact of torque-split controller. The graph shows that using torque-split control with two EM (170 kW and 30 kW maximum power), the energy consumption is reduced by 30% and 18% for UDDS and US06, respectively, compared to the architecture with one EM (200 kW maximum power).

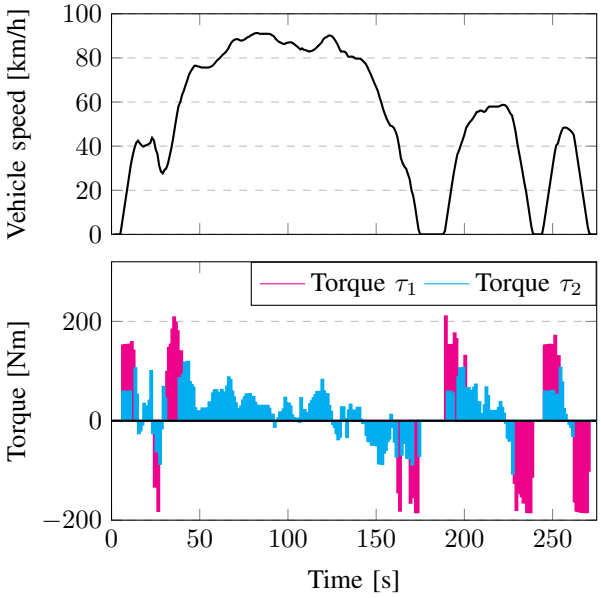

Fig. 3. Illustration of torque-split controller. Top: Segment of UDDS vehicle speed trajectory. Bottom: Torques τ_1 and τ_2 provided by EM 1 (max. power 150 kW) and EM 2 (max. power 50 kW), respectively. The plot shows how a torque-split controller operates by using EM 2 for low-torque demand, EM 1 for high-torque demand, and both EM 1 with EM 2 for peak torque demand.

that an EV architecture with a 170 kW and a 30 kW motor works well for both UDDS and US06. Fig. 3 illustrates how the energy-optimal control algorithm in this paper splits the torque demand between the two motors.

Impact of torque-split and CVT controller: Fig. 4 shows the combinations of a two EM architecture with and without CVTs. Energy savings are displayed in reference to an EV with one motor without CVTs. The most promising architecture is a two-EM architecture with a CVT connected to the weaker motor. Intuitively, this makes sense as the vehicle operates at low-torque demand for the majority of time, e.g., cruise conditions. Adding a second CVT to the more powerful motor does not yield an advantage, because the added weight makes the EV less efficient overall. The peak savings are around 39% and 20% for UDDS and US06 cycles, respectively. For comparison, we also included the

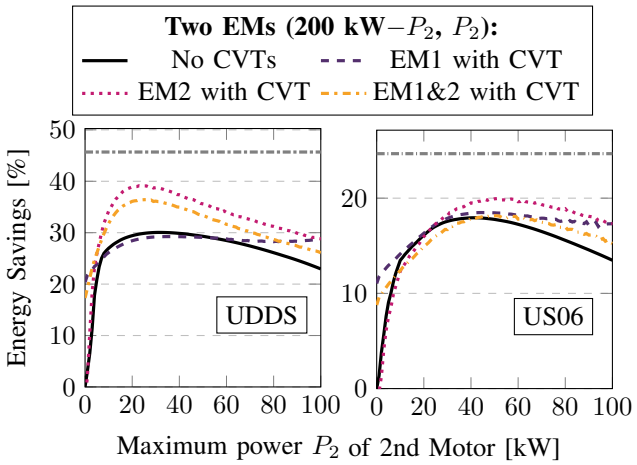

Fig. 4. Energy savings compared to baseline configuration (one EM with 200 kW, fixed gear). Left: Urban driving schedule. Right: Highway driving schedule. The hypothetical maximum savings are illustrated as dash-dotted constant in gray and result from operating the EV at maximum efficiency.

maximum hypothetical energy savings that the EV would achieve if it could operate its motor with maximum efficiency at all times, $\eta_{\text{opt}} = \max_{\omega,\tau}(\eta(\omega,\tau))$.

B. Velocity Profile Optimization

Next, we consider the joint velocity profile optimization and EM control problem. Compared to the results in Section IV-A, this provides an additional degree of freedom in the form of the velocity profile that can be used to further reduce the energy consumption of the EV.

In order to illustrate the algorithm in this paper, we present two acceleration tasks, in which the EV accelerates from the initial velocities 10 km/h and 20 km/h to reach 60 km/h and 100 km/h, respectively, within 30 s. Indeed, it is beneficial not to simply use a constant acceleration profile, but take motor efficiencies into consideration instead. In order to obtain a fair comparison, we constrain the average velocity such that the distance traveled over 30 s is the same. We use $T_s = 0.5$ s, $N_{\text{VP}} = 60$, and the constraints for the velocity profile optimization in (11), $c_{\text{profile,eq}}(v_k, a_k) = v_{N_{\text{VP}}} - v_{\text{end}} = 0$, and $c_{\text{profile,eq}}(v_k, a_k) = \frac{v_{\text{end}} - v_0}{2} - \frac{1}{N_{\text{VP}}} \sum_{k=1}^{N_{\text{VP}}} v_k \leq 0$, where the former constrains the end velocity and the latter constrains the average velocity. Other constraints for the velocity profile optimization can be easily included.

Table II summarizes energy savings for the velocity profile optimization. The energy savings are computed in reference to a constant acceleration profile, which also uses the torque-split and the CVT controller (Lines 7–9 in Algorithm 1) so that the saved energy is entirely achieved by the modulation of acceleration. Fig. 5 shows the velocity profiles resulting from the four EV architectures. It shows that the energy-optimal velocity profile depends on the configuration. For example, for the EV without a CVT, it is optimal to first accelerate using the more powerful EM 1 (see left plot 0–8 s; right plot 0–9 s), then switch to the less powerful EM 2 (see left plot 8–26 s; right plot 9–22 s), and switch back to

TABLE II

ENERGY SAVINGS - OPTIMIZED VELOCITY PROFILE

Motor 1 170 kW	Motor 2 30 kW	Accelerate in 30 s initial – end velocity	Energy Savings
Fixed gear	Fixed gear	10 – 60 km/h 20 – 100 km/h	5.4% 5.2%
CVT	Fixed gear	10 – 60 km/h 20 – 100 km/h	13.0% 7.3%
Fixed gear	CVT	10 – 60 km/h 20 – 100 km/h	1.5% 4.6%
CVT	CVT	10 – 60 km/h 20 – 100 km/h	1.5% 4.4%

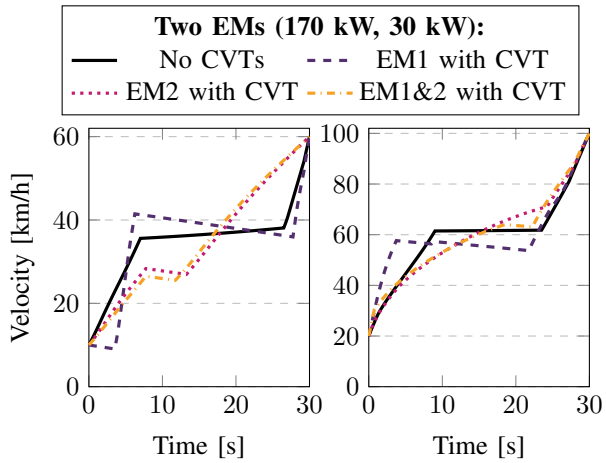

Fig. 5. Velocity profile resulting from optimization.

the more powerful EM 1 (see left plot 26–30 s; right plot 22–30 s). Using the velocity profile computed in Line 6 in Algorithm 1 rather than a constant acceleration profile, the EV can save 1.5–13% depending on the EV configuration.

Remark 7: The computation times for the velocity profile optimization using cost functions as in Fig. 1 ranged from 0.02 s to 0.1 s, which is well below the 0.5 s sampling time used here. The computation times for the torque-split and the transmission controller are around 1 ms. We used a gradient-descent solver and backtracking line search implemented in MATLAB with no code optimization and hence with major possible improvements. We used a MacBook Pro with 2 GHz Quad-Core Intel Core i5 and 32 GB 3733 MHz RAM.

V. CONCLUSION

This paper presented an algorithm for energy-optimal control of EVs with multiple motors and/or CVTs. The control algorithm uses kernel regression in order to learn a pseudo-convex cost function from motor efficiency data. It is implemented in a sequential three-steps control algorithm. First, a energy-optimal velocity profile is generated. Second, the optimal torque-split ratio between the multiple motors is computed using the velocity profile. Third, the optimal gear ratio is computed using the torque-split ratio and the velocity profile. The method offers low computation times due to the pseudo convexity. Simulation results using the UDDS and US06 driving schedules show energy savings potential up to 20–40% compared to an EV with one specific EM. Furthermore, simulation results of an acceleration task show that energy-optimal velocity profile optimization can save up to an additional 13% energy.

REFERENCES

[1] L. Guzzella and A. Amstutz, "QuasiStatic Simulation Toolbox." https://idsc.ethz.ch/research-guzzella-onder/downloads.html. Accessed: 2021-01-01.

[2] A. Sciarretta, M. Back, and L. Guzzella, "Optimal control of parallel hybrid electric vehicles," *IEEE Transactions on Control Systems Technology*, vol. 12, no. 3, pp. 352–363, 2004.

[3] A. Sciarretta and L. Guzzella, "Control of hybrid electric vehicles," *IEEE Control Systems Magazine*, vol. 27, no. 2, pp. 60–70, 2007.

[4] D. Ambühl, *Energy management strategies for hybrid electric vehicles*. PhD thesis, ETH Zurich, 2009.

[5] H. Borhan, A. Vahidi, A. M. Phillips, M. L. Kuang, I. V. Kolmanovsky, and S. Di Cairano, "MPC-based energy management of a power-split hybrid electric vehicle," *IEEE Transactions on Control Systems Technology*, vol. 20, no. 3, pp. 593–603, 2012.

[6] S. Di Cairano, D. Bernardini, A. Bemporad, and I. V. Kolmanovsky, "Stochastic MPC with learning for driver-predictive vehicle control and its application to HEV energy management," *IEEE Transactions on Control Systems Technology*, vol. 22, no. 3, pp. 1018–1031, 2014.

[7] T. Nüesch, P. Elbert, M. Flankl, C. Onder, and L. Guzzella, "Convex optimization for the energy management of hybrid electric vehicles considering engine start and gearshift costs," *Energies*, vol. 7, no. 2, pp. 834–856, 2014.

[8] P. Elbert, T. Nuesch, A. Ritter, N. Murgovski, and L. Guzzella, "Engine on/off control for the energy management of a serial hybrid electric bus via convex optimization," *IEEE Transactions on Vehicular Technology*, vol. 63, no. 8, pp. 3549–3559, 2014.

[9] S. Ebbesen, M. Salazar, P. Elbert, C. Bussi, and C. H. Onder, "Time-optimal control strategies for a hybrid electric race car," *IEEE Transactions on Control Systems Technology*, vol. 26, no. 1, pp. 233–247, 2018.

[10] H. Wang, Y. Huang, A. Soltani, A. Khajepour, and D. Cao, "Cyber-physical predictive energy management for through-the-road hybrid vehicles," *IEEE Transactions on Vehicular Technology*, vol. 68, no. 4, pp. 3246–3256, 2019.

[11] S. Di Cairano, W. Liang, I. V. Kolmanovsky, M. L. Kuang, and A. M. Phillips, "Power smoothing energy management and its application to a series hybrid powertrain," *IEEE Transactions on Control Systems Technology*, vol. 21, no. 6, pp. 2091–2103, 2012.

[12] Y. Zhou, A. Ravey, and M.-C. Péra, "A survey on driving prediction techniques for predictive energy management of plug-in hybrid electric vehicles," *Journal of Power Sources*, vol. 412, pp. 480–495, 2019.

[13] R. Wang, H. Zhang, and J. Wang, "Linear parameter-varying controller design for four-wheel independently actuated electric ground vehicles with active steering systems," *IEEE Transactions on Control Systems Technology*, vol. 22, no. 4, pp. 1281–1296, 2014.

[14] A. Ritter, P. Elbert, and C. Onder, "Energy saving potential of a battery-assisted fleet of trolley buses," *IFAC-PapersOnLine*, vol. 49, no. 11, pp. 377–384, 2016.

[15] L. Gang and Y. Zhi, "Energy saving control based on motor efficiency map for electric vehicles with four-wheel independently driven in-wheel motors," *Advances in Mechanical Engineering*, vol. 10, no. 8, pp. 1–18, 2018.

[16] Y. Gao, W. Wang, and Y. Li, "Optimization of control strategy for dual-motor coupling propulsion system based on dynamic programming method," in *2019 3rd Conference on Vehicle Control and Intelligence (CVCI)*, 2019.

[17] D. Chen, C. Danielson, and M. Iezawa, "Improving passenger comfort by exploiting hub motors in electric vehicles: Suspension modeling," in *Dynamic Systems and Control Conference*, vol. 84287, 2020.

[18] Q. Zheng, S. Tian, and Q. Zhang, "Optimal torque split strategy of dual-motor electric vehicle using adaptive nonlinear particle swarm optimization," *Mathematical Problems in Engineering*, pp. 1–21, 2020.

[19] C. E. Rasmussen and C. K. I. Williams, *Gaussian Processes for Machine Learning*. The MIT Press, 2006.

[20] United States Environmental Protection Agency, "Dynamometer Drive Schedules." https://www.epa.gov/vehicle-and-fuel-emissions-testing/dynamometer-drive-schedules. Accessed: 2021-01-01.